

# SOME PROBLEMS RELATED TO THE ESTABLISHMENT OF EARTHQUAKE DESIGN FORCE LEVELS

A.T. Derecho and M. Iqbal

## SYNOPSIS

Selected problems associated with the determination of design force levels for use in earthquake-resistant design are presented. Design force levels considered are those pertaining particularly to isolated reinforced concrete structural walls. The approach adopted involves a correlation of results from comprehensive dynamic inelastic analyses and data from tests of large-size specimens subjected to slowly reversed loading.

Among the problems discussed are those relating to the determination of critical response values, with special reference to the choice of input motions. Also considered is the choice of an adequate measure of inelastic deformation from among several alternative measures proposed in the literature. Finally the problem of correlating force demands obtained from dynamic inelastic analyses with capacity values determined from tests of large-size specimens subjected to slowly reversed loading is discussed.

## RESUME

Les problèmes choisis associés au niveau de force pour le calcul des constructions antisismiques se rapportent aux murs individuels de béton armé travaillant en flexion. Ces problèmes comprennent la détermination des valeurs des réponses critiques, faisant particulièrement référence au choix des mouvements du sol et au choix d'une mesure adéquate de la déformation inélastique parmi diverses définitions possibles proposées dans la documentation. Finalement le problème de la corrélation des forces obtenues des analyses inélastiques dynamiques ayant des valeurs de capacité déterminées à partir d'essai de spécimens de grande dimension qui sont soumis à des charges en "va-et-vient" appliquées lentement est discuté.

Arnaldo T. Derecho obtained his his Ph.D. from the University of Illinois, Urbana, in 1966. He is currently Manager, Structural Analytical Section, Portland Cement Association, Skokie, Illinois. He is the author of numerous publications on the behavior of structures under lateral loads and is a member of ACI Committee 442, Response of Structures to Lateral Loads.

Mohammad Iqbal obtained his D.Sc. from Washington University, St. Louis, Missouri, in 1973. He is currently Senior Structural Engineer in the Structural Analytical Section, Portland Cement Association, Skokie, Illinois. He is the author or coauthor of several papers and is involved in research on the behavior of structures under wind and earthquakes.

#### INTRODUCTION

In developing design procedures for earthquake-resistant structures, information on demand as well as on capacity has to be developed. As indicated in Fig. 1, this information relates mainly to stiffness, strength and inelastic deformation capacity or ductility. Except for the addition of inelastic deformation capacity, these are no different from the design considerations for gravity and wind loading. Economy in engineering design makes it desirable to establish reasonable estimates of both demand and capacity under specific conditions.

While it is not too difficult to accumulate data on expected loads for gravity and wind loading from actual measurements, the same cannot be said of earthquake-induced forces. The relative infrequency of intense earthquakes makes accumulation of data on earthquake demands a difficult task. Furthermore, there is the low likelihood that a building exposed to an intense earthquake will be adequately instrumented to record its response.

In view of the difficulty of obtaining sufficient data on earthquake demands from field measurements, at present the next best alternative is to obtain estimates of these demands through dynamic inelastic analysis. Estimates of capacity are usually obtained by testing large-size specimens under slowly reversed loading to simulate earthquake response.

Problems discussed in this report were encountered in the process of developing design procedures for earthquake-resistant reinforced concrete structural walls and wall systems. This investigation is part of a combined analytical and experimental program supported in major part by Grant No. ENV77-15333 from the National Science Foundation.

The initial phase of the investigation considers isolated structural walls. Isolated walls were considered first not only to obtain dynamic response data on this basic element but also to establish a reference with which results for the more complex structural wall systems, to be considered in the subsequent phase, can be compared. This paper is limited to the work on isolated structural walls.

The general problem considered in the investigation is the determination of design force levels corresponding to a broad range of values of significant structural parameters and ground motion intensities. Forces obtained can then be used to analyze and design structures using static analysis procedures. The second major part of the design procedure involves establishing detailing requirements to provide the necessary capacity to members subjected to known forces. The second part is based primarily on experimental results and will not be discussed here.

A brief description of the general approach followed in the analytical investigation is given below. This is followed by a discussion of selected aspects of technical interest considered in the investigation.

#### BASIC APPROACH

The approach adopted in establishing design force levels for earthquake-resistant isolated structural walls involved compilation of comprehensive inelastic response data for a wide range of values of the significant structural and ground motion parameters. For simplicity it was felt essential to base the procedure for determining design force levels on a few most important parameters.

Identification of the most important parameters for use in the design formulation required a parametric investigation (1). Included in this investigation was a study of the effects on dynamic inelastic response of the three major parameters characterizing earthquake ground motions. These parameters are intensity, duration, and frequency content. Also considered were fundamental period, yield level in flexure, the ratio of post-yield stiffness to initial elastic stiffness, parameters characterizing the moment-rotation hysteretic loop, damping, stiffness and strength taper along height of structure, number of stories, and base fixity. The computer program DRAIN-2D (2), developed at the University of California, Berkeley, was used in the analyses.

Results of the parametric study showed that, within the practical range of values of the variables considered, the most significant structural parameter are fundamental period and yield level in flexure. The major ground motion parameter is intensity.

Once the major variables affecting inelastic dynamic response had been identified, an extensive series of analyses was carried out. Over 300 such analyses were performed. The aim was to compile response data corresponding to a wide range of values of the major

variables. These data were then organized, evaluated and correlated with relevant experimental data to develop a procedure for determining design force levels.

To provide background, a brief description of the procedure developed for determining design force levels for isolated structural walls is presented. More detailed material is given in Ref. 3. The procedure is best explained with reference to Figs. 2 through 5. These figures show the general form of plots of critical response data and experimental results used in the procedure.

The charts shown in Figs. 2, 3, and 4 correspond to a specific ground motion intensity. Earthquake intensity is expressed in terms of "spectrum intensity", defined in this study as the area under the 5%-damped relative velocity response spectrum associated with the first 10 seconds of an accelerogram. The spectrum intensity for the N-S component of the 1940 El Centro record was used as the reference intensity,  $SI_{ref.}$ . The plots shown in Figs. 2, 3, and 4 correspond to an input motion with intensity equal to  $1.5 SI_{ref.}$ .

The procedure for determining design force levels consists mainly of the following steps:

1. Starting with a preliminary design satisfying gravity and wind loading requirements, assume an available rotational ductility,  $\mu_r^a$ . An estimate may be obtained by using a chart based on experimental data (4,5) similar to the plot shown in Fig. 5, by entering the chart with an estimate of the design nominal shear stress.
2. Determine the flexural design factor,  $\alpha_f$ , from a chart such as is shown in Fig. 2. Using the flexural design factor,  $\alpha_f$ , the flexural reinforcement required to provide the minimum yield level,  $M_y^{\min}$ , at the base of the wall can be determined (see Fig. 6). Provision of  $M_y^{\min}$  at the critical section will ensure that the available rotational ductility assumed in Step (1) is not exceeded under the design earthquake intensity.
3. Determine the shear design factor,  $\alpha_v$ , from a chart similar to that shown in Fig. 3. Using  $\alpha_v$ , and a reduction factor, an "effective static shear"\* can be calculated.
4. Check if the available ductility,  $\mu_r^a$ , assumed in Step (1) can be developed under the design shear stress corresponding to the shear determined in Step (3) above. This check can be

\*This is an equivalent static design shear value obtained by applying a multiplier to the calculated critical dynamic shears to account for the effect of a number of factors and allow a comparison with shear strength values obtained experimentally under slowly reversed loading.



done using a chart such as shown in Fig. 5, based on experimental data.

If the assumed ductility can be developed, then determine the required shear reinforcement. This will be based on design recommendations based on results of the experimental program (4,5).

5. If the assumed ductility cannot be developed under the calculated design shear stress, adjust the assumed ductility value accordingly and repeat Steps (1) through (4) until reasonable agreement between assumed and developable ductilities is obtained.

The above steps cover the design of the critical region at the base of an isolated structural wall. Specifically considered are the forces necessary to determine flexural and shear reinforcement. Assumed as known or specified are the fundamental period of the structure and the design earthquake intensity.

A major distinction between the proposed procedure and current simplified design procedures is the explicit relationship established between the principal structural parameters and the force and deformation requirements corresponding to a particular earthquake intensity. Also important is the manner in which these have been correlated with experimental data to yield design forces. A design procedure for frame-wall systems can be developed along similar lines, with appropriate modifications to reflect the effect of other structural parameters characterizing the more complex systems.

In the process of developing data for the above procedure, certain important questions had to be considered. Among the problems involved which will be discussed below are those relating to (a) the determination of critical response values, with special reference to the choice of input motions, (b) the choice of an adequate measure of inelastic deformation demand and capacity from a number of alternative measures proposed in the literature, and (c) the correlation of demands determined from inelastic dynamic analysis with capacities obtained from tests under slowly reversing loads, with special reference to shear.

#### CRITICAL INPUT MOTIONS

Because of the variability of the character of the ground motion at a particular site, it is desirable to base estimates of dynamic response for design purposes on a number of input motions reflecting probable characteristics expected at the site. In compiling critical or near-maximum response data for structures with different fundamental periods and yield levels, it was necessary to limit the number of input motions used to a minimum. To accomplish this, a study was made of the major parameters characterizing input motions. The immediate object of this examination was to enable a selection of critical input motions for particular structures on the basis of these parameters.

Three major parameters characterize input motions, namely, intensity, duration, and frequency content. Intensity is a measure of the amplitude of the acceleration pulses, particularly as it affects structural response. An examination of several measures (6) indicates that spectrum intensity, as defined earlier, provides a reasonably good index of intensity. Some measure of intensity is usually specified or implied in the provisions of codes for design purposes, corresponding to different levels of seismic risk.

Examination of recorded accelerograms (6) indicates that the strong phases of most occur within the first 10 to 15 seconds of the motion. In terms of response, the major effect of an increase in duration of the strong phases of a ground motion is an increase in cumulative inelastic deformation demand. Analyses carried out during this investigation showed that maximum response quantities, except cumulative response quantities, were not significantly affected by an increase in input motion duration.

The importance of knowing the frequency characteristics of a given input motion lies in the phenomenon of resonance or near-resonance. This occurs when the frequency of the exciting force or motion approaches the frequency of the structure. Near-maximum response to earthquake excitation can be expected if the dominant frequency components occur in the same frequency range as the dominant effective frequencies of the structure.

A convenient way of studying the frequency characteristics of an accelerogram is provided by the Fourier amplitude spectrum. This spectrum provides a frequency decomposition of the accelerogram, indicating the amplitude (in units of velocity - a measure of the energy content) of the component at a particular frequency. Another commonly used measure of the frequency content of an accelerogram is the velocity response spectrum. This is a plot showing the variation of the maximum absolute value of the relative velocity of a linear single-degree-of-freedom system with the undamped natural period (or frequency) when subjected to a particular input motion. Figure 7 from Ref. 7, shows velocity response spectra for the N-S component of the 1940 El Centro record, for different values of the damping factor. The dashed curve in Fig. 7 is the corresponding Fourier amplitude spectrum. As in the Fourier spectrum, the peaks in the velocity response spectrum reflect concentrations of the input energy at or near the corresponding frequencies.

Although both Fourier amplitude and undamped velocity response spectra exhibit a jagged character, it is usually possible to recognize a general trend in the overall shape of any particular curve. By noting the general shape of the spectrum in the frequency range of interest, a characterization of the input motion in terms of frequency content can be made.

In this study, a viscous damping coefficient of 5% of critical for the first mode was used as the basic value for the dynamic analysis model. Accordingly, the 5%-damped velocity response spectra cor-

responding to the first 10 seconds of a large number of selected records were examined. On the basis of this examination, two general categories, shown in Fig. 8, were recognized:

1. A "peaking" accelerogram with a spectrum exhibiting dominant frequencies over a well-defined period range. The N-S component of the 1940 El Centro record is an example of this class.
2. A "broad-band" accelerogram that has a more or less flat spectrum over the period range of interest. The vertical component of the 1940 El Centro record falls into this category. A sub-class of the broad-band category is a record with a spectrum which increases with increasing period within the period range of interest. This may be referred to as an "ascending" accelerogram. The E-W component of the 1940 El Centro record is typical of this type of record.

The above proposed classification of accelerograms in terms of frequency content represents a rather crude method and does not account for the variation of frequency content with time (8). Nevertheless, it provides a sufficient basis for determining the potential severity of a given input motion in relation to a specific structure.

#### Frequency Content and Structural Response

For a linear structure in which dynamic behavior is dominated by the fundamental mode, strong response can be expected when the fundamental period falls within the peaking range of the input motion. This happens when the period range of the dominant components of the input motion is similar to those of the structure. A weaker response can be expected if the dominant period of the structure falls outside the peaking range.

For isolated walls where only nominal yielding occurs, the initial fundamental period may continue to provide a good approximation of the effective period of the structure even after yielding. This is also true for highly redundant structures such as frames and frame-wall systems where yielding in some elements may not significantly change the effective period of the structure. For these cases, a peaking accelerogram with its spectrum peak centered about the initial fundamental period will likely produce a more severe response than a broad-band accelerogram of the same intensity.

The effective period of a yielding structure changes with the extent of inelastic action and the general state of deformation of the structure. Thus, different components of an input motion will exert varying influences on the behavior of the structure at different times. Since the general effect of yielding is to increase the period of vibration, the longer-period components in a record will tend to play a greater role as yielding progresses in the structure.

### Verification of Frequency Content Classification

To verify the above observation on the effects of "peaking" and "broad-band" accelerograms, dynamic analyses were carried out on isolated structural wall models. The analyses were done using the program DRAIN-2D (2). Three sets of analyses were made, as described in Table 1. Five of the six accelerograms shown in Fig. 9 were used for this particular study. The corresponding 5%-damped velocity spectra are shown in Fig. 10.

The isolated structural wall considered in the analyses is assumed to form part of a hypothetical 20-story building consisting of a series of parallel walls, as shown in Fig. 11. The moment-rotation relationship for the wall is characterized by a decrease in the reloading stiffness with increasing deformations beyond yield, as shown in Fig. 12 (9). To save on computer time with little sacrifice in accuracy of results, the 12-mass model shown in Fig. 11c was selected after some preliminary analyses. A discussion of results for the three sets of data listed in Table 1 is given below.

Set (a). Envelopes of response values for a structure with a period of 1.4 sec. and a yield level,  $M_y = 500,000$  in.-kips (56,490 kN m), are shown in Fig. 13. Figures 13a and c indicate that the E-W component of the 1940 El Centro record, classified as "broad-band ascending", produces relatively greater maximum displacements and ductility requirements than the other three input motions considered. However, the same record produces the least value of the maximum horizontal shear.

It is significant to note that as yielding progresses and the effective period increases, it is the "broad-band ascending" type of accelerogram (in this case, the El Centro E-W component) that excites the structure most severely. Response to the other types of accelerogram, particularly the peaking accelerograms, are less severe. An indication of the change in fundamental period of a structure as the hinging region progresses from the first story upward is given by Fig. 14, for different values of the yield stiffness ratio,  $r_y$ . This figure is based on properties of a structure with initial fundamental period,  $T_1 = 1.4$  sec.

Set (b). To determine the effects of frequency characteristics for short-period structures with relatively high yield levels, a "peaking" accelerogram, the N-S component of the 1940 El Centro, was considered. For this set, a structure with fundamental period,  $T_1 = 0.8$  sec. and a yield level,  $M_y = 1,500,000$  in.-kips (169,470 kN m), was assumed.

Figure 15 shows response envelopes for this set. As can be seen, the peaking accelerogram consistently produces a greater response in the structure than a broad-band record. A comparison of Fig. 15c and Fig. 13c indicates that the ductility requirements are significantly less for this structure with a high yield level. In addition, yielding does not progress as high up the wall as in the case of the structure with period  $T_1 = 1.4$  sec. and a low yield level.

The greater response of the structure under the N-S component of the 1940 El Centro (peaking) follows from the fact that the dominant frequency components for this motion occur in the vicinity of the period of the structure. In this region the E-W component has relatively low-powered components. Also, because of the high yield level of the structure, yielding was not extensive, particularly under the E-W component.

Set (c). In the third set, the same structure considered in Set (a) was used but with the intensity of ground motion reduced by one-half. The two motions used were the 1971 Pacoima Dam, S16E record, a peaking motion, and the 1940 El Centro, E-W, a broad-band record.

Calculated envelopes of response are shown in Fig. 16. These support the observation that when yielding in a structure is not extensive enough to cause a significant increase in the effective period, a peaking type accelerogram is likely to produce the more critical response. Figure 16c shows that in this case, yielding in the structure does not extend far above the base when compared to Set (a) where the input motion was twice as intense. It will be noted that in Set (a), the broad-band 1940 El Centro, E-W motion with intensity equal to 1.5 ( $SI_{ref.}$ ) represented the critical motion, while the Pacoima Dam record, a peaking motion, produced a relatively smaller response. By reducing the intensity of the motions by one-half so that yielding in the structure is significantly reduced, the Pacoima Dam record becomes the more critical motion, as Fig. 16 shows.

Summary. The extent of yielding in a structure is influenced by the yield level,  $M_y$ , as well as the intensity of the input motion. For this reason, both parameters should be taken into account when selecting the appropriate type of motion to use as input, with particular reference to frequency characteristics.

Thus, where inelastic deformation is limited, due to a low intensity ground motion or a high structure yield level, an accelerogram with a peaking type velocity spectrum tends to be more critical than a broad-band motion of the same intensity and duration. On the other hand, where extensive yielding occurs in a structure, due either to a high intensity ground motion or a low structure yield level, the broad-band type accelerogram is likely to be the more critical motion.

The above criteria for selecting the critical input motion apply insofar as lateral displacements and rotational ductilities are concerned. This correlation reflects the dominant influence of the fundamental mode on these response quantities. They do not, however, seem to apply to the selection of critical motions with respect to base shear, particularly where significant yielding occurs. The maximum base shears are affected more significantly by higher mode response.

## AN ADEQUATE MEASURE OF INELASTIC DEFORMATION

Another interesting problem encountered in the process of developing a procedure for determining design force levels for earthquake-resistant walls relates to measures of inelastic deformation. In comparing deformation demand determined by analysis with capacity values obtained from tests, several measures may be considered. Figure 17 shows some of the measures that have been used for maximum rotation and cumulative rotational deformation.

It is of major practical interest to determine if a comparison of demand and capacity based on a single measure of deformation is possible. This would simplify the design procedure considerably.

In this study it is assumed that the hinging region, i.e., the segment of wall where most of the inelastic flexural deformation occurs, extends vertically from the base a distance approximately equal to the width of the wall. This is indicated in Fig. 18. Under this assumption, the nodal rotation at the upper limit of the assumed hinging length represents the total rotation in that length.

Measures of Inelastic Deformation Considered

Using the base moment-nodal rotation ( $M-\theta$ ) curves as basic data, the following measures of deformation requirement (and capacity) for the hinging region near the base of the wall were considered (see Fig. 17):

- (a) Rotational ductility,  $\mu_r$ , is the ratio of the maximum nodal rotation measured from the zero-rotation axis,  $\theta_{max}$ , to the corresponding nodal rotation,  $\theta_y$ , when the moment at the base first reaches the yield moment,  $M_y$ .
- (b) Cyclic rotational ductility,  $\mu_{rc}$ , is the ratio of the maximum absolute nodal rotation measured from the point where the  $M-\theta$  curve intersects the zero-moment axis,  $\theta_{max}^c$ , to  $\theta_y$ .
- (c) Cumulative rotational ductility,  $\Sigma\mu_{rc}$ , is the cumulative sum of the absolute values of the nodal rotations for the entire duration of the response divided by the yield rotation,  $\theta_y$ .
- (d) Cumulative rotational energy,  $\Sigma A_r$ , is the cumulative sum of the areas under the individual  $M-\theta$  hysteretic loops for the entire duration of the response divided by  $M_y\theta_y/2$ .

It is obvious that maximum deformation alone does not sufficiently describe the deformation demand associated with dynamic seismic response. Information on maximum deformation must be supplemented by data on the number of cycles of large-amplitude (comparable to the maximum) deformation. This is important since the behavior of structures loaded in the inelastic range can be significantly affected by the number of cycles of large amplitude imposed. A good indication

of the number of large-amplitude cycles is provided by the cumulative measures of deformation described above and shown in Fig. 17.

By noting the relationship between measures of deformation demand as indicated by dynamic analyses and comparing these with the corresponding ratios for the laboratory specimens, it was possible to identify a single, readily determinable, parameter for use in correlating deformation demand with capacity.

As a first step in evaluating data, plots of maximum values of the above measures of deformation were prepared. Figures 19 and 20 show representative maximum deformation curves for the case of 20-story isolated walls with  $M_y = 750,000$  in.-kips (84,750 kN m). A curve was plotted corresponding to each of the six accelerograms shown in Fig. 9. Most of the analyses were carried out using a duration of 10 seconds and an intensity equal to 1.5 ( $SI_{ref.}$ ). The cumulative measures have been adjusted to reflect a 20-second duration of the input motions.

From the plots of maximum response values due to different input motions, a second set of curves was prepared showing only the critical values of the response quantities corresponding to different combinations of fundamental period and yield level. Figures 21 through 24 show critical plots of the measures of deformation considered for the case of 20-story isolated walls. A curve in Figs. 21, for instances, is defined by points representing the largest ductility values from among several maximum response curves such as shown in Figs. 19. Points determining a curve in Figs. 21 through 24 can thus correspond to different input motions. The procedure followed in developing the critical response plots is described in greater detail in Ref. 3.

#### Check on Adequacy of Rotational Ductility as a Measure of Inelastic Deformation

To assess the adequacy of each of the measures of ductility as a representative index of deformation demand, a comparison with corresponding measures of capacity obtained from tests was undertaken. Adequacy of a measure, in this context, implies that a comparison based on this measure will yield conclusions that are also applicable to the other measures of deformation.

The comparison undertaken here involves ratios of each of the measures of deformation to a specific "reference measure". In this case, rotational ductility was used as the reference measure. Ratios of deformation demands from the analytical investigation are compared with corresponding ratios of deformation capacity from tests. The experimental data considered are results from the concurrent experimental investigation (4,5).

Relative Magnitudes of Measures of Deformation Demand. To obtain an indication of the relative magnitudes of the different measures of deformation demand representing critical dynamic response, Figs. 25 to 27 were prepared. These figures present data for 20-story structural walls subjected to input motions with intensity  $SI = 1.5$



( $SI_{ref.}$ ). In these figures, the variation of the ratio of each measure of deformation to  $\mu_{r2}$  with the fundamental period is shown for different values of the reference measure  $\mu_{r2}$ . The subscript "2" in  $\mu_{r2}$  serves to indicate that it is based on the nodal rotation at the second floor level. The distribution of the plotted points does not appear to indicate a dependence of the different ratios on either the fundamental period or the value of the reference measure,  $\mu_{r2}$ .

Figure 25 shows the average ratio of critical cyclic rotational ductility to the critical rotational ductility,  $\mu_{rc2}/\mu_{r2}$ , to be 1.2. The ratio of the cumulative rotational ductility to rotational ductility,  $\Sigma\mu_{rc2}/\mu_{r2}$ , varies from about 13.5 to 20.2, with a mean value of 16.2, as shown in Fig. 26. The ratio of cumulative rotational energy to rotational ductility,  $\Sigma A_{r2}/\mu_{r2}$ , on the other hand, varies from about 5.8 to 14.6, with the mean value of 11.8, as shown in Fig. 27.

A plot showing all three ratios discussed above is shown in Fig. 28.

#### Experimental Investigation

The experimental investigation (4,5) is an integral part of the overall project. It is aimed at developing procedures for the design of structural walls to provide the strength and deformation capacity indicated by dynamic response studies.

During the first phase of the experimental investigation, isolated structural walls of various configurations were constructed and tested. Details of the specimens and the test procedure are given in Refs. 4 and 5. Out of the 16 tests reported, one was conducted under monotonic loading and 2 were retests of repaired specimens that had been tested earlier. Results of 13 tests form the basis for the comparison discussed in this section.

Ductilities of Test Specimens. The rotational ductility,  $\mu_r$ , cyclic rotational ductility,  $\mu_{rc}$ , cumulative rotational ductility,  $\Sigma\mu_{rc}$ , and cumulative rotational energy,  $\Sigma A_{rc}$ , were computed from data for each of the test specimens considered. These measures of deformation are based on the measured rotation of a section about 74 in. above the base. This height is approximately equal to the width of the specimens. Most of the inelastic deformation in the walls tested was confined to the first 6 ft at the base of the walls.

The rotational ductility,  $\mu_r$ , of the hinging region at the ultimate deformation stage for each of the thirteen test specimens are plotted against the corresponding nominal shear stress in Fig. 29. The dashed line drawn in this figure represents a lower bound to the plotted points. Any point on this line indicates the minimum rotational ductility that, according to the test results, is available under the nominal shear stress which corresponds to the point.



Figures 30, 31 and 32 are plots of the cyclic rotational ductility,  $\mu_{RC}$ , cumulative rotational ductility,  $\Sigma\mu_{RC}$ , and cumulative rotational energy,  $\Sigma A_{RC}$ , respectively, against the maximum applied nominal shear stress. All these measures correspond to the hinging region of the test specimens.

The dashed line in Fig. 30 represents a magnification of values corresponding to the dashed line in Fig. 29 by a factor of 1.5. In other words, for the same value of the nominal shear stress, the dashed line of Fig. 30 would yield a cyclic rotational ductility,  $\mu_{RC}$ , equal to 1.5 times the corresponding rotational ductility,  $\mu_r$ . It can be seen that the dashed line of Fig. 30 constitutes a lower bound to the plotted points. This means that for the same nominal shear stress a minimum cyclic rotational ductility equal to 1.5 times the minimum available rotational ductility can be counted on.

The dashed lines in Figs. 31 and 32 similarly represent magnifications of the values corresponding to the dashed line in Fig. 29 by factors of 22.0 and 21.0, respectively.

The dashed lines in Figs. 30, 31 and 32 indicate that if a minimum rotational ductility,  $\mu_r$ , of 3, say, is available under a particular nominal shear stress, a minimum cyclic rotational ductility of  $3 \times 1.5 = 4.5$ , a minimum cumulative ductility of  $3 \times 22 = 66$ , and a minimum cumulative rotational energy of  $3 \times 21 = 63$  are also available.

By noting the relative magnitudes of the different measures of available ductility in terms of a reference measure (in this case,  $\mu_r$ ), a comparison with the corresponding quantities representing ductility demands can conveniently be made.

#### Comparison of Measures of Demand and Capacity

Figure 33 shows a comparison of the different measures of deformation demand with corresponding measures of capacity.

Data points representing demand in Fig. 33 are based on the maximum ratios from Figs. 25 to 27. Points representing capacity are ratios associated with the lower-bound curves of Figs. 30 to 32. In Fig. 33 and in the subsequent discussion, the subscript "2" attached to the symbols for measures of deformation demand have been dropped for convenience. It is apparent from Fig. 33 that the demand in terms of the three ratios based on  $\mu_r$ , is less than the corresponding available capacity. Thus, if the ductility requirements are satisfied in terms of  $\mu_r$ , they will automatically be satisfied in terms of the other three measures of inelastic deformation.

Summary. A comparison of deformation demand and capacity was carried out, using several measures of inelastic deformation. The comparison was made in terms of ratios of selected measures of deformation to a reference measure. In this case, the reference measure used was rotational ductility,  $\mu_r$ . The primary purpose of the

comparison was to determine if it is possible to base a comparison of demand and capacity on only one measure of deformation.

Although the data considered is limited, the above comparison provides a strong indication of the adequacy of rotational ductility,  $\mu_r$ , as a measure of deformation demand and capacity. This means that satisfaction of ductility requirements in terms of  $\mu_r$  automatically implies satisfaction of the same requirements in terms of the other three measures of ductility. Because  $\mu_r$  is the most conveniently determined measure among the four measures considered, and one that has been widely used in the literature, it was decided to adopt it as the basic measure of deformation demand and capacity.

In comparing the measures of deformation demand obtained from dynamic analysis with deformation capacity from laboratory tests, it was implicitly assumed that the test conditions corresponded to the response of isolated walls to 20-second input motions having an intensity equal to 1.5 ( $SI_{ref.}$ ).

Another important assumption made in carrying out the above comparisons concerns the effect of loading history. It was assumed that the behavior of reinforced concrete walls subjected to reversed cyclic loading is not significantly affected by differences between tests and analyses with respect to the number of cycles of large-amplitude deformations or the sequence in which these large deformations were imposed on the specimens. This question requires further investigation to more fully establish the validity of the preceding comparison (10).

#### EFFECT OF CHARACTER OF SHEAR LOADING

In the procedure developed for determining design force levels, capacity values obtained from experiments are correlated with demands estimated through dynamic inelastic analyses. It is essential, in this respect, that the capacity values be derived under conditions closely approximating dynamic conditions. This is particularly important for conditions or factors that have significant influence on the behavior of reinforced concrete structures. The validity of any correlation between demand and capacity will depend on how representative the loading conditions used in the laboratory are of actual dynamic response. While there are many aspects to this problem (11), only one will be discussed here.

In simulating earthquake response through tests of specimens under slowly reversed loading, it is important to recognize differences between this type of loading and that under dynamic response conditions. Some of these differences may significantly affect the comparison of capacity values obtained from tests with estimates of demand based on dynamic analysis. Where a significant difference affecting structural behavior is noted, allowance for this difference should be provided by adjusting either capacity or demand values before a comparison is made. The case of shear will be considered here. This is an important question because of the significant

influence that shear can have on structural behavior under cyclic loading with large deformations.

As far as the shear force used in tests is concerned, two aspects have to be considered. First is the magnitude of the maximum shear force. The second is its variation with time, and particularly in relation to the accompanying moment and deformation. Most of the quasi-static tests that have been conducted to date have been concerned mainly with the magnitude of the expected shear forces. The loading imposed on test specimens has been characterized by the moment, shear and the deformation in the critical region being all in phase. This results from the application on a specimen of one or more horizontal forces in the same direction which are varied proportionally.

Response studies of isolated structural walls undertaken in this investigation indicate that the shear in the critical region at the base is more sensitive to higher mode response. Thus, it fluctuates more rapidly with time than either moment or rotation. This is illustrated in Fig. 34 which show time-history plots of the shear, rotation and moment in the first story of an isolated wall subjected to two different input motions. It is believed that a loading condition in which the shear force fluctuates relatively rapidly with respect to moment and rotation represents a less severe loading than that used in quasi-static tests. Under typical dynamic conditions, the shear attains its peak value only for very short durations. In quasi-static tests, on the other hand, the shear, moment and rotation are all in phase and are sustained over a longer duration. However, the significance of these effects can be determined only through a series of tests using an earthquake simulator (shaking table). The question is of sufficient importance to merit early resolution, particularly in view of the high shear forces indicated by analysis (3) relative to present code values.

#### GENERAL SUMMARY

Questions arising in the process of developing a procedure for determining design force levels for earthquake-resistant reinforced concrete isolated structural walls are reviewed and the approaches taken to resolve some of these discussed.

On the problem of determining critical input motions for use in developing design data, attention was focused on the frequency characteristics of the ground motion. A classification of accelerograms based on the shape of the associated 5%-damped velocity response spectrum is proposed. Using this classification, it is shown that where inelastic action is limited, an accelerogram with a 'peaking' type velocity spectrum tends to be more critical than a 'broad-band' motion of the same intensity and duration. On the other hand, where extensive yielding occurs in a structure, the broad-band type accelerogram is more likely to be critical. These observations apply particularly to the effect of frequency content on displacements and ductilities. These quantities are heavily influenced by the fundamental period of the structure. The maximum base shear, however, is

more sensitive to higher modes of response. Because of this, the criteria developed for selecting critical input motions for displacement, base moment and ductility do not necessarily apply with respect to shear. This is particularly true where significant yielding occurs.

The second problem considered is that of determining a single measure of inelastic deformation in the critical region that can adequately represent both maximum as well as cumulative deformations. Using such a measure, deformation demand and capacity can be compared and conclusions made in relation to this measure would automatically apply to the other measures of deformation. Results of this study have shown that rotational ductility, defined as the ratio of the maximum rotation in the hinging region to the corresponding yield rotation, provides an adequate measure.

The third problem discussed relates to the difference in the character of the shear loading occurring in dynamic response and that used in slowly reversed loading tests to simulate earthquake response. The possible difference in effect on structural behavior of a rapidly changing shear force such as occurs under dynamic conditions and that of a loading where moment, shear and rotation are all in phase is pointed out. The resolution of this important question is proposed as a subject for future investigation.

#### ACKNOWLEDGEMENT

Work on this investigation was supported in major part by Grant No. ENV77-15333 from the National Science Foundation. The investigation is part of a project on "Structural Walls in Earthquake-Resistant Buildings." Any opinions, findings and conclusions expressed in this report are those of the authors and do not necessarily reflect the views of the National Science Foundation.

The review of the paper by Dr. W. G. Corley, Director, Engineering Development Department, Portland Cement Association, is gratefully acknowledged.

#### REFERENCES

1. Derecho, A.T., Ghosh, S.K., Iqbal, M., Freskakis, G.N. and Fintel, M., "Structural Walls in Earthquake-Resistant Buildings - Analytical Investigation, Dynamic Analysis of Isolated Structural Walls - PARAMETRIC STUDIES," Final Report to the National Science Foundation, RANN, under Grant No. ENV74-14766, Portland Cement Association, March 1978.
2. Kanaan, A.E. and Powell, G.H., "General Purpose Computer Program for Dynamic Analysis of Plane Inelastic Structures," (DRAIN-2D), Report No. EERC 73-6, Earthquake Engineering Research Center, University of California, Berkeley, April 1973.

3. Derecho, A.T., Iqbal, M., Fintel, M. and Corley, W.G., "Structural Walls in Earthquake-Resistant Buildings - Analytical Investigation, Dynamic Analysis of Isolated Structural Walls - DEVELOPMENT OF DESIGN PROCEDURE - DESIGN FORCE LEVELS," Final Report to the National Science Foundation, RANN, under Grant No. ENV74-14766, Portland Cement Association, April 1979.
4. Oesterle, R.G., Fiorato, A.E., Johal, L.S., Carpenter, J.E., Russell, H.G. and Corley, W.G., "Earthquake-Resistant Structural Walls - Tests of Isolated Walls," Report to the National Science Foundation, Portland Cement Association, November 1976, 44 pp. (Appendix A, 38 pp.; Appendix B, 233 pp.)
5. Oesterle, R.G., Aristizabal, J.D., Fiorato, A.E., Russell, H.G. and Corley, W.G., "Earthquake-Resistant Structural Walls - Tests of Isolated Walls - Phase II," Report to the National Science Foundation, Portland Cement Association, November 1977.
6. Derecho, A.T., Fugelso, L.E. and Fintel, M., "Structural Walls in Earthquake-Resistant Buildings - Analytical Investigation, Dynamic Analysis of Isolated Structural Walls - INPUT MOTIONS," Final Report to the National Science Foundation, RANN, under Grant No. ENV74-14766, Portland Cement Association, January 1978.
7. Analysis of Strong Motion Earthquake Accelerograms, Vol. III-Response Spectra, Part A-Accelerograms HA001 through HA030, Report EERL 72-80, California Institute of Technology, Earthquake Engineering Research Laboratory, August 1972.
8. Saragoni, G.R. and Hart, G.C., "Time Variation of Ground Motion Frequency Content: Characterization and Relevance," Proceedings of the Fifth World Conference on Earthquake Engineering, Rome, 1973, Session 4A, Paper No. 156.
9. Takeda, T., Sozen, M.A. and Nielsen, N.N., "Reinforced Concrete Response to Simulated Earthquake," Journal of the Structural Division, ASCE, Proceedings, Vol. 96, No. ST12, December 1970.
10. Derecho, A.T., Iqbal, M., Ghosh, S.K., Fintel, M., and Corley, W.G., "Structural Walls in Earthquake-Resistant Buildings - Analytical Investigation, Dynamic Analysis of Isolated Structural Walls - REPRESENTATIVE LOADING HISTORY," Final Report to the National Science Foundation, RANN, under Grant No. ENV74-14766, Portland Cement Association, March 1978.
11. Bertero, V.V., "Identification of Research Needs for Improving Aseismic Design of Building Structures," Report No. EERC 75-27, University of California, Berkeley, September 1975.

Table 1 - Summary of Input Motions Considered in Study of Frequency Characteristics

Set	Structure Period, $T_1$ (and $M_y$ )	Input Motion	Frequency Content Characterization	Intensity Normalization Factor
a	1.4 sec. (500,000 in.-k)	1971 Pacoima Dam, SIGE component	Peaking (0)	0.59
		1971 Holiday Inn Orion, E-W component	Peaking (+)	3.22
		Artificial Accelerogram, S1	Broad band	1.65
		1940 El Centro, E-W component	Broad band, ascending	1.88
b	0.8 sec. (1,500,000 in.-k)	1940 El Centro, N-S component	Peaking (0)	1.50
		1940 El Centro, E-W component	Broad band, ascending	1.88
c	2.0 sec. (500,000 in.-k)	1971 Holiday Inn, Orion, E-W component	Peaking (-)	3.22
		1940 El Centro, E-W component	Broad band, ascending	1.88
		Artificial Accelerogram, S1	Broad band	1.65

1 in.-kip = 0.11298 kN.m

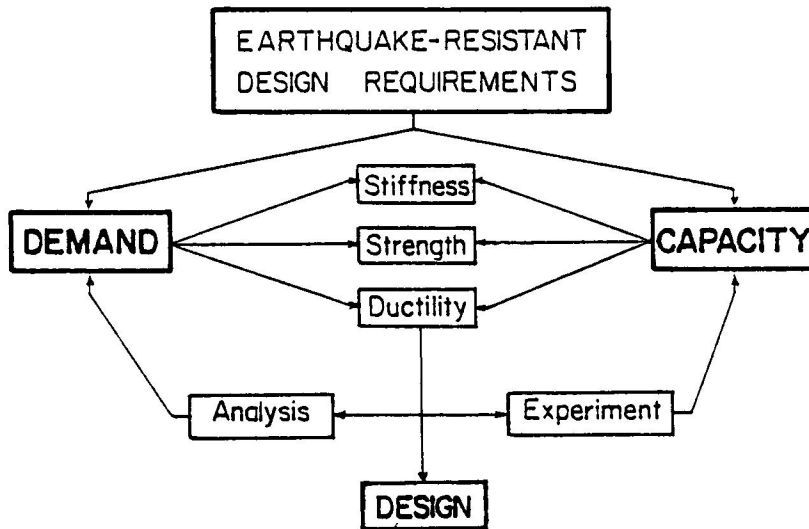


Fig. 1 Basic Elements of Earthquake-Resistant Design

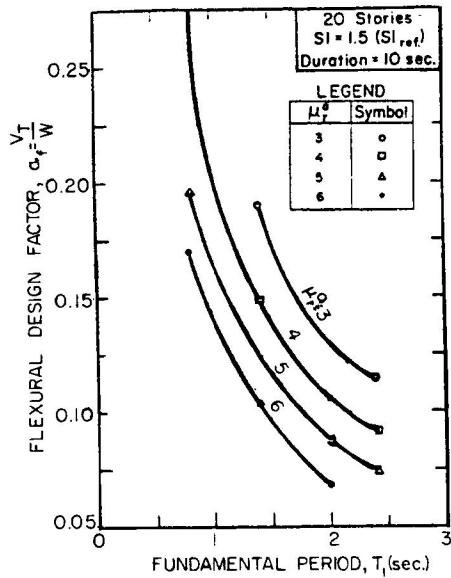


Fig. 2 Flexural Design Factor,  $\alpha_f$ , as a Function of Available Rotational Ductility,  $\mu_f^a$ , and Fundamental Period,  $T_1$

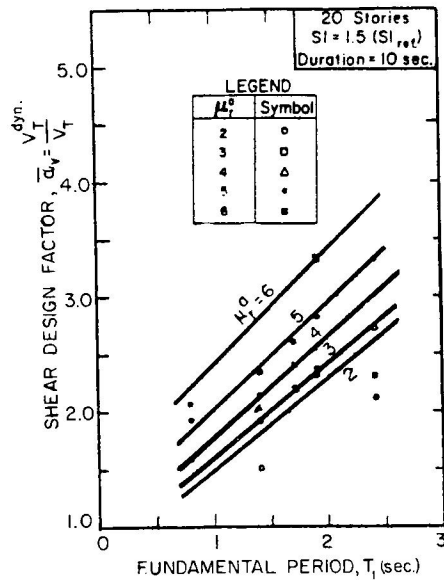


Fig. 3 Shear Design Factor,  $\alpha_v$ , as a Function of Available Rotational Ductility,  $\mu_f^a$ , and Fundamental Period,  $T_1$

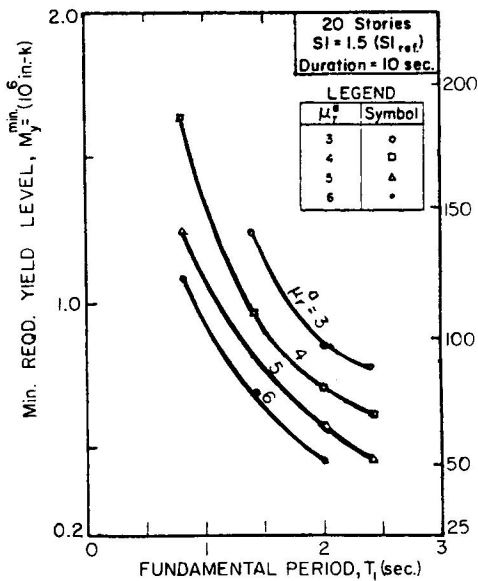


Fig. 4 Minimum Yield Level,  $M_y^{\min}$ , Required at Base as a Function of Available Rotational Ductility,  $\mu_f^a$ , and Fundamental Period,  $T_1$

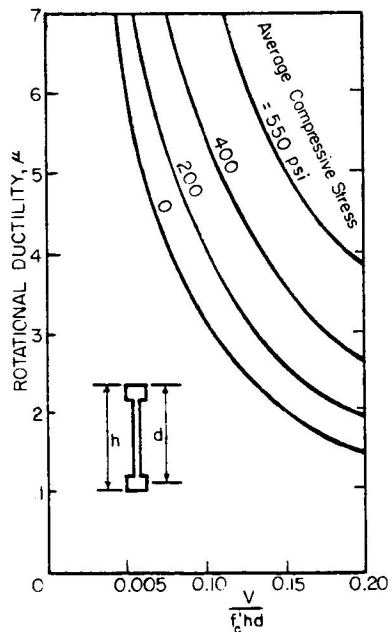


Fig. 5 Rotational Ductility Ratio,  $\mu_r$ , as a Function of Maximum Nominal Shear Strees-Isolated Wall Specimens

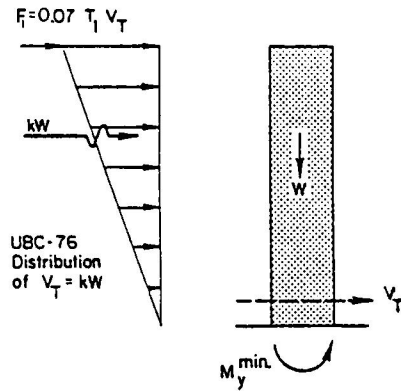


Fig. 6 Distribution of Lateral Forces Along the Height of Isolated Structural Walls

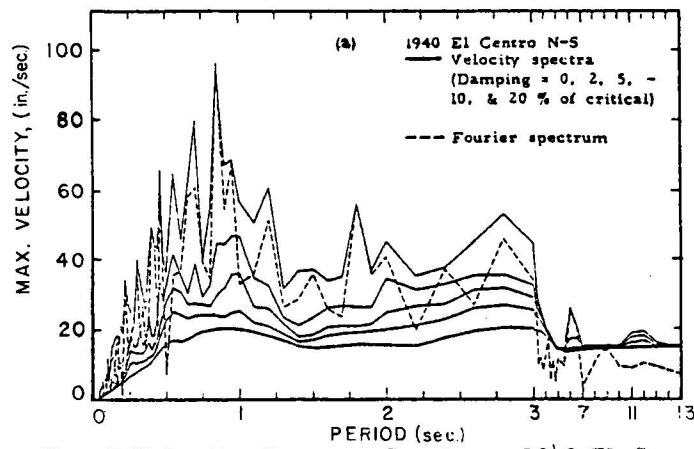


Fig. 7 Velocity Response Spectra - 1940 El Centro, N-S Component (from Ref. 7)



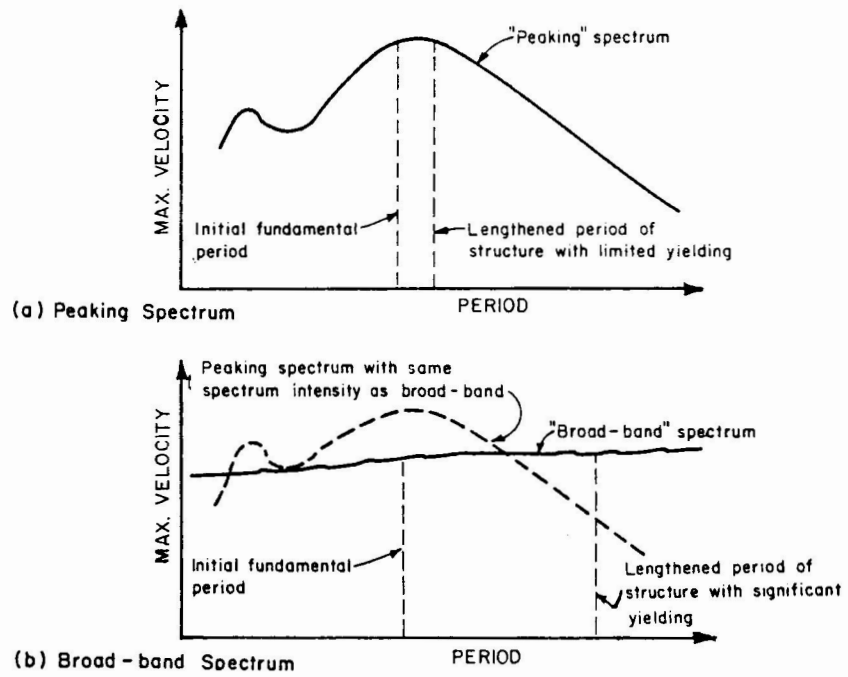


Fig. 8 Typical Basic Shapes of Damped Velocity Response Spectra

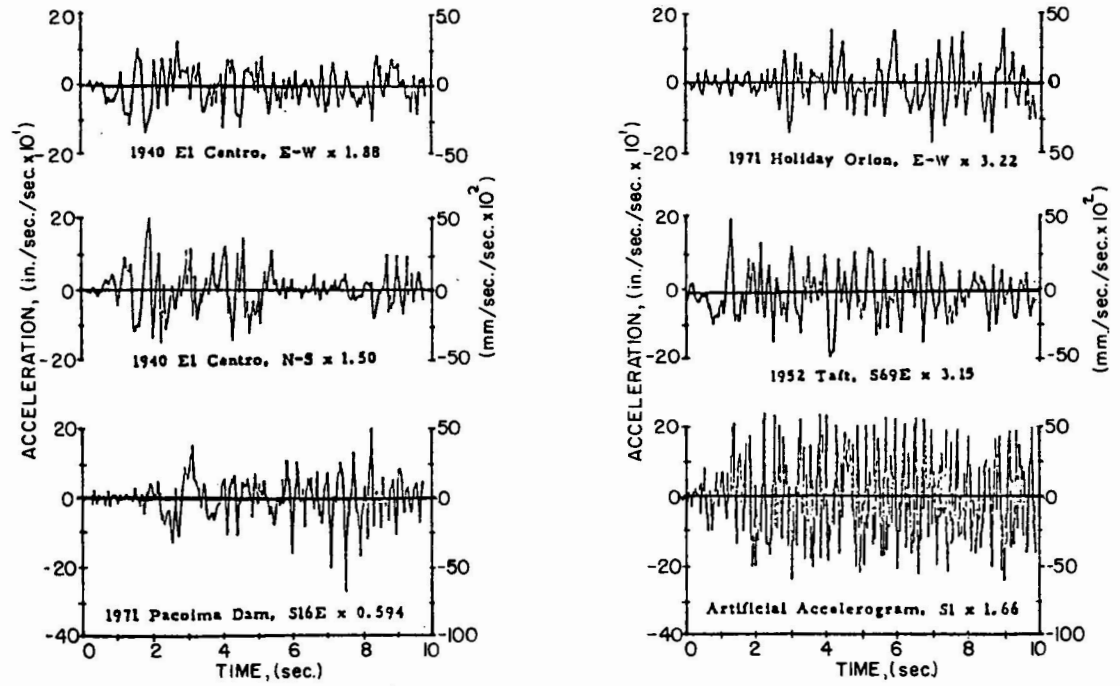


Fig. 9 Ten-Second Duration Normalized Accelerograms

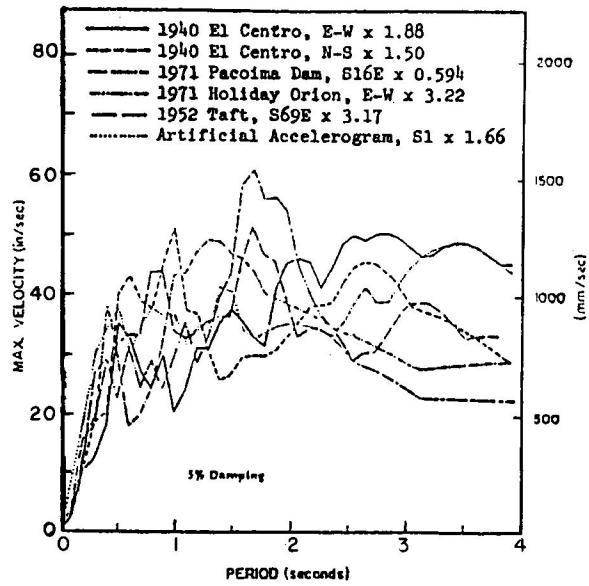


Fig. 10 Relative Velocity Response Spectra for First Ten Seconds of Normalized Input Motions

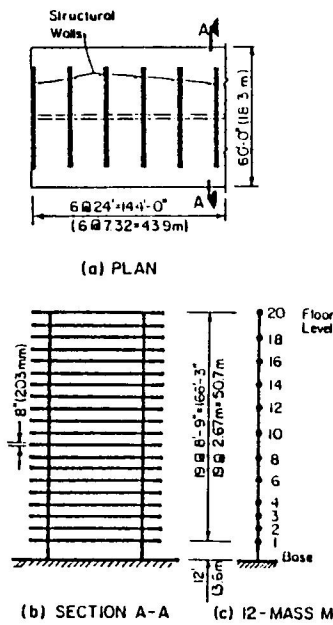


Fig. 11 Twenty-Story Building with Isolated Structural Walls and Analytical Model of Wall

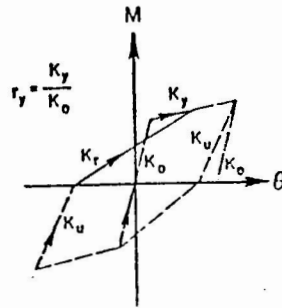


Fig. 12 Modified Takeda Decreasing Stiffness Model for Hinging Regions

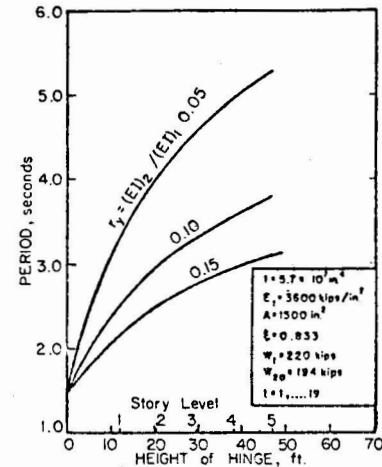


Fig. 14 Fundamental Period versus Height of Yield Hinge, 20-Mass Cantilever

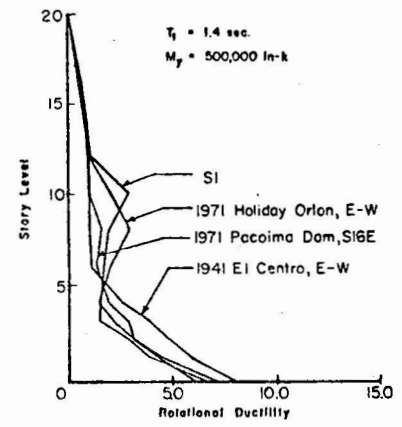
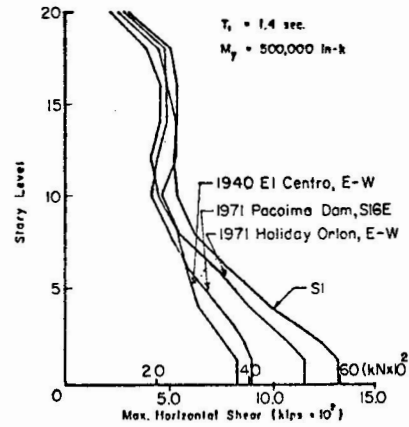
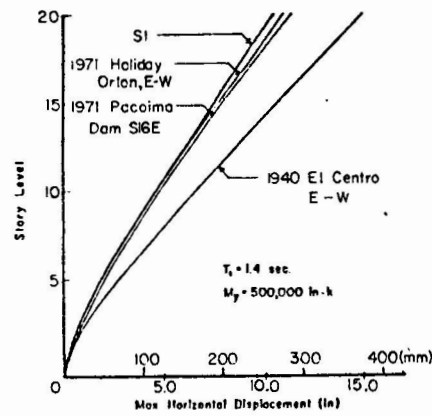


Fig. 13 Effect of Frequency Characteristics of Ground Motion - Structure with Low Yield Level

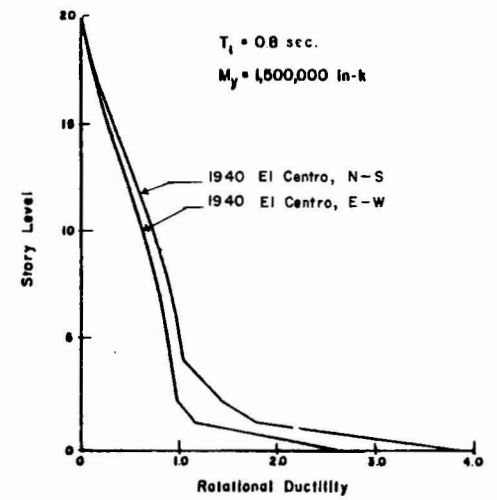
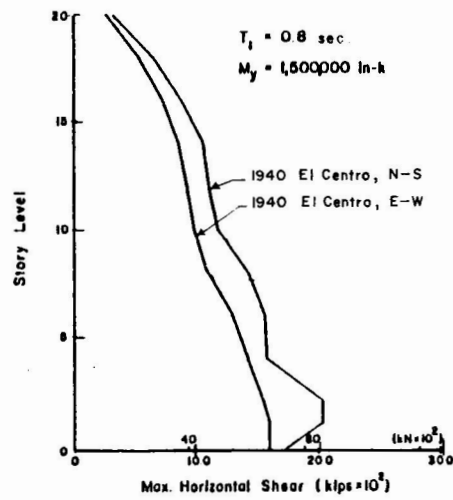
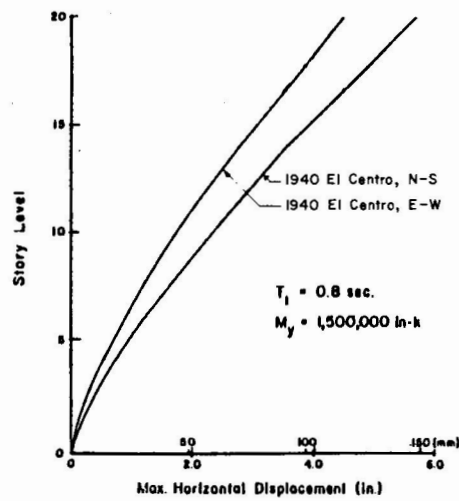


Fig. 15 Effect of Frequency Characteristics of Ground Motion - Structure with High Yield Level

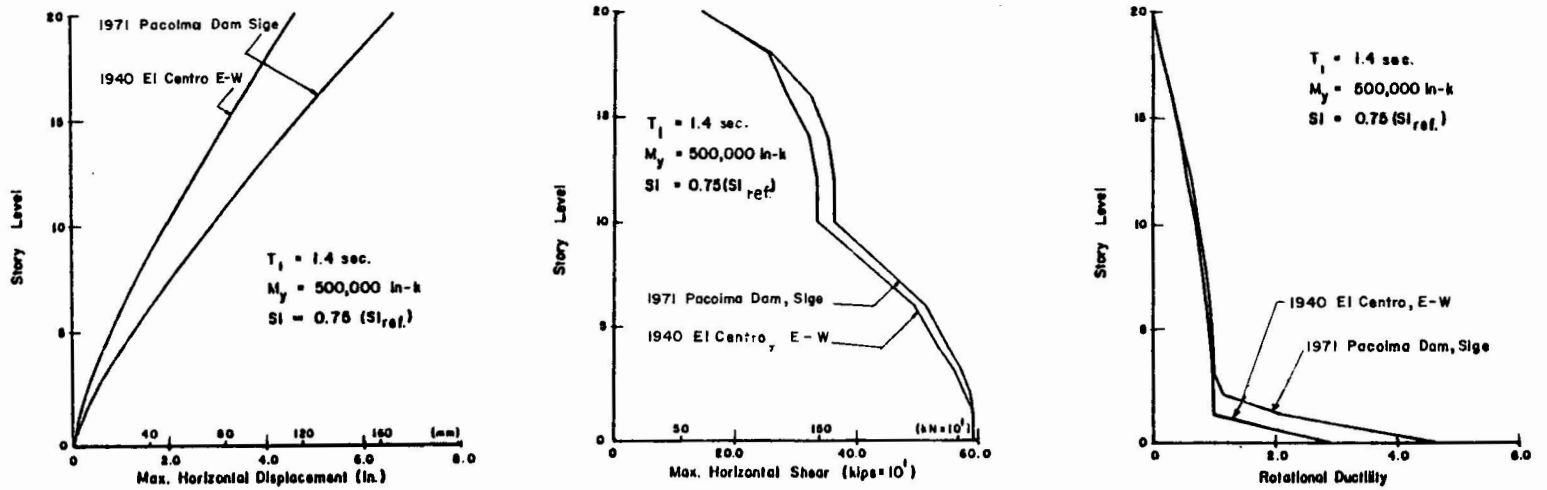
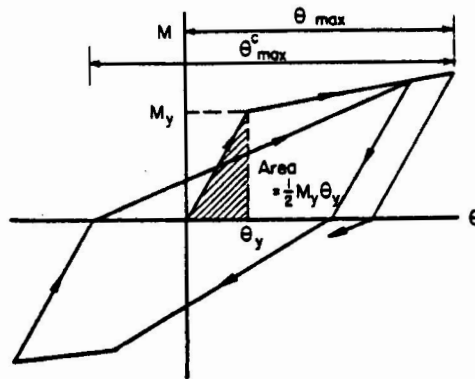


Fig. 16 Interacting Effects of Input Motion Intensity and Frequency Characteristics and Structure Yield Level



rotational ductility,  $\mu_r = \frac{\theta_{max}}{\theta_y}$

cyclic rotational ductility,  $\mu_{rc} = \frac{\theta_{max}^c}{\theta_y}$

cumulative rotational ductility =  $\sum \mu_{rc} = \frac{\sum \theta_{max}^c}{\theta_y}$

cumulative rotational energy, =  $\sum A_r = \frac{\text{cumulative area under } M-\theta \text{ loops}}{\frac{1}{2} M_y \theta_y}$

Fig. 17 Measures of Inelastic Flexural Deformation in Hinging Region

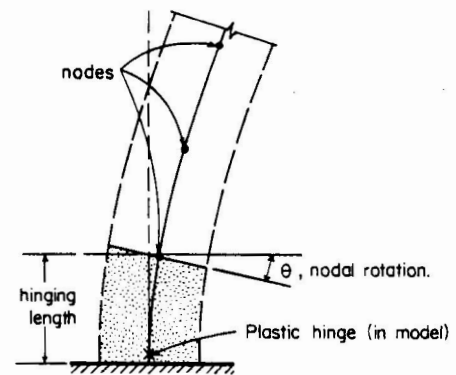


Fig. 18 Nodal Rotation as a Measure of Flexural Deformation in Hinging Region

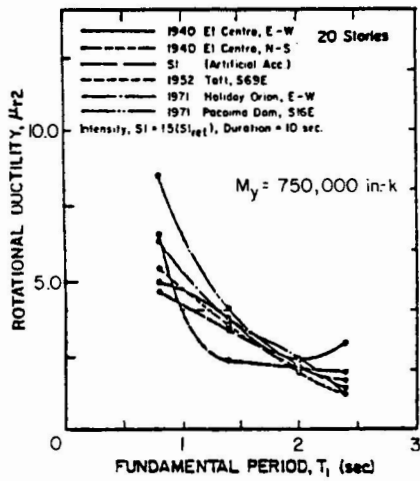


Fig. 19 Maximum Rotational Ductility,  $\mu_{r2}$  for Different Input Motions

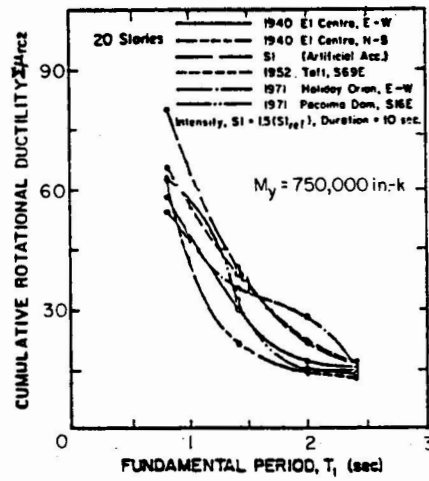


Fig. 20 Cumulative Rotational Ductility,  $\epsilon_{rc2}$  for Different Input Motions

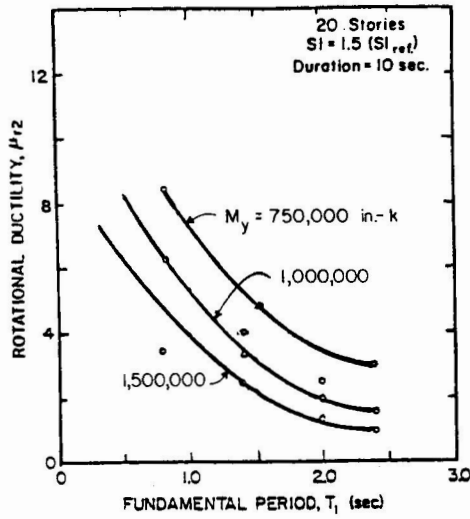


Fig. 21 Critical Rotational Ductility,  $\mu_{r2}$ , as a Function of  $T_1$  and  $M_y$

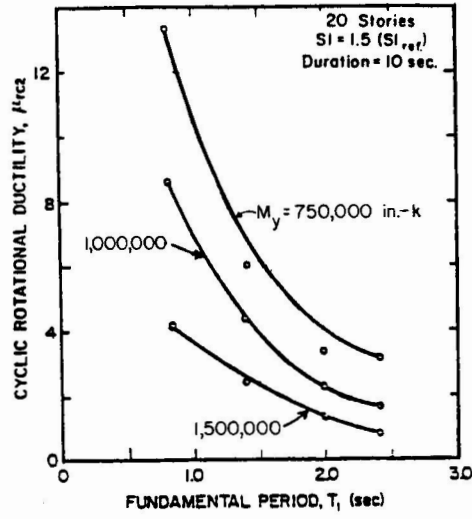


Fig. 22 Critical Cyclic Rotational Ductility,  $\mu_{rc2}$ , as a Function of  $T_1$  and  $M_y$



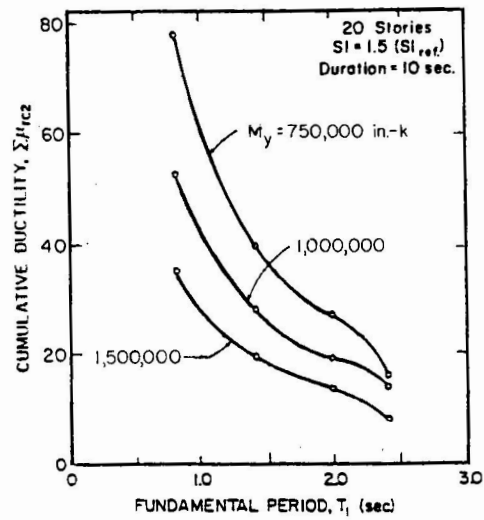


Fig. 23 Critical Cumulative Ductility,  $\Sigma \mu_{rc2}$ , as a Function of  $T_1$  and  $M_y$

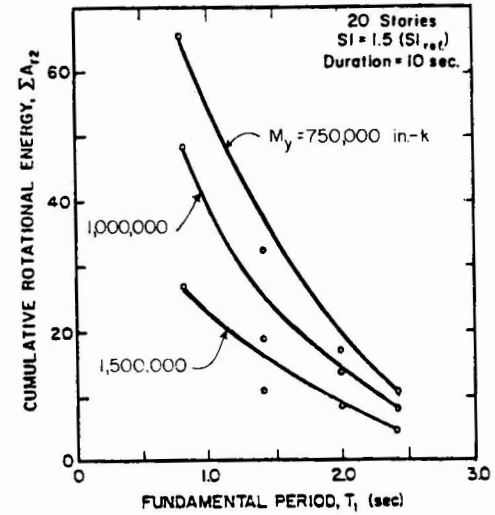


Fig. 24 Critical Cumulative Energy,  $\Sigma A_{r2}$ , as a Function of  $T_1$  and  $M_y$

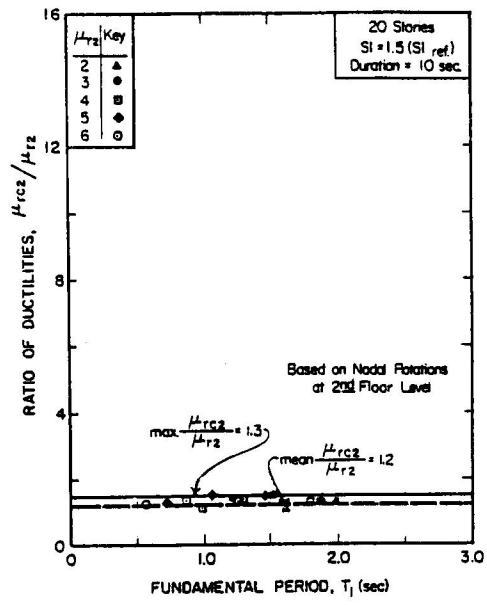


Fig. 25 Ratio of Cyclic Rotational Ductility,  $\mu_{rc2}$ , to Rotational Ductility,  $\mu_{r2}$

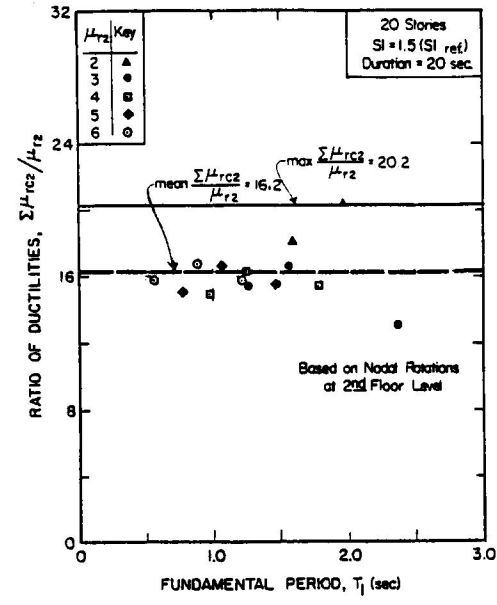


Fig. 26 Ratio of Cumulative Rotational Ductility,  $\Sigma\mu_{rc2}$ , to Rotational Ductility,  $\mu_{r2}$

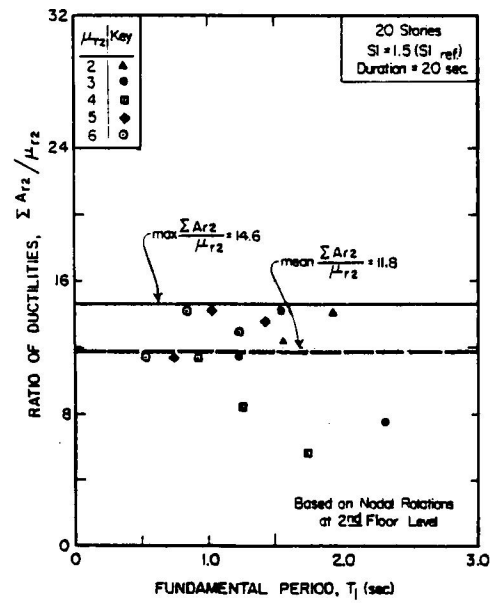


Fig. 27 Ratio of Cumulative Rotational Energy,  $\Sigma A_{r2}$ , to Rotational Ductility,  $\mu_{r2}$

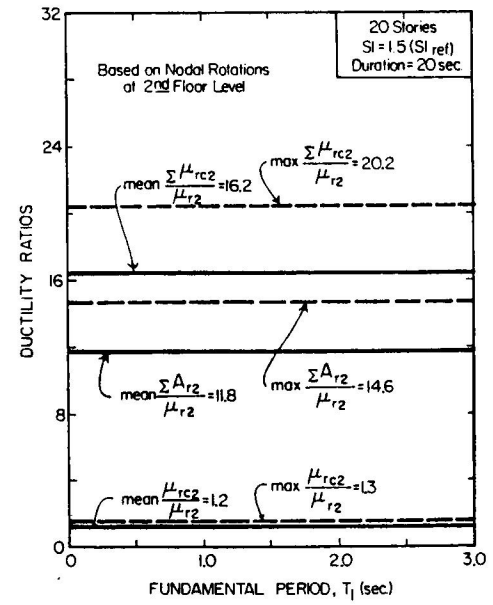


Fig. 28 Summary of Ductility Ratios Based on Rotational Ductility,  $\mu_{r2}$

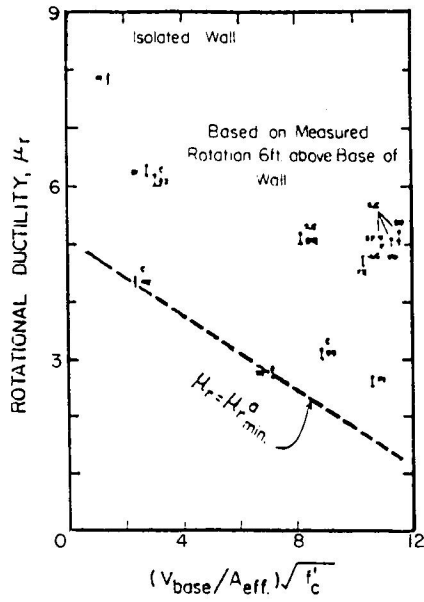


Fig. 29 Rotational Ductility  $\mu_r$ , Versus Maximum Nominal Shear Stress

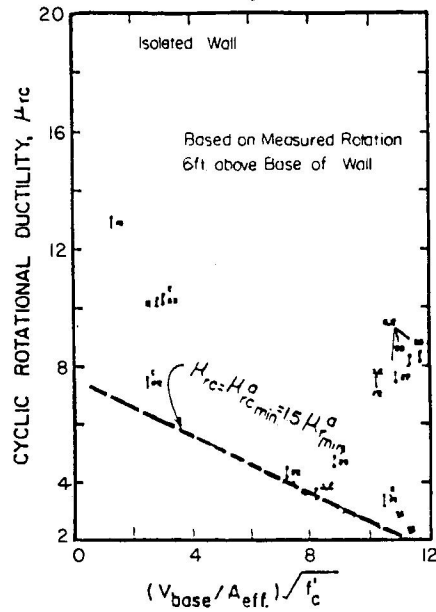


Fig. 30 Cyclic Rotational Ductility Ratio,  $\mu_{rc}$ , versus Maximum Nominal Shear Stress

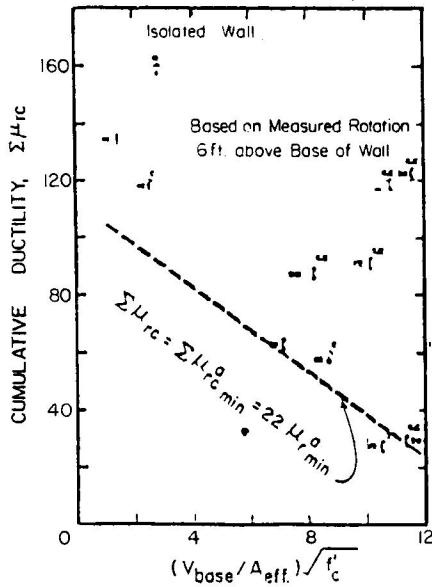


Fig. 31 Cumulative Rotational Ductility,  $\Sigma\mu_{rc}$ , versus Maximum Nominal Shear Stress

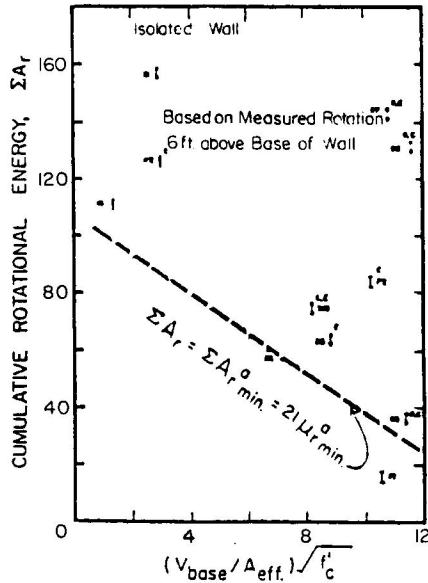


Fig. 32 Cumulative Rotational Energy,  $\Sigma A_r$ , versus Maximum Nominal Shear Stress

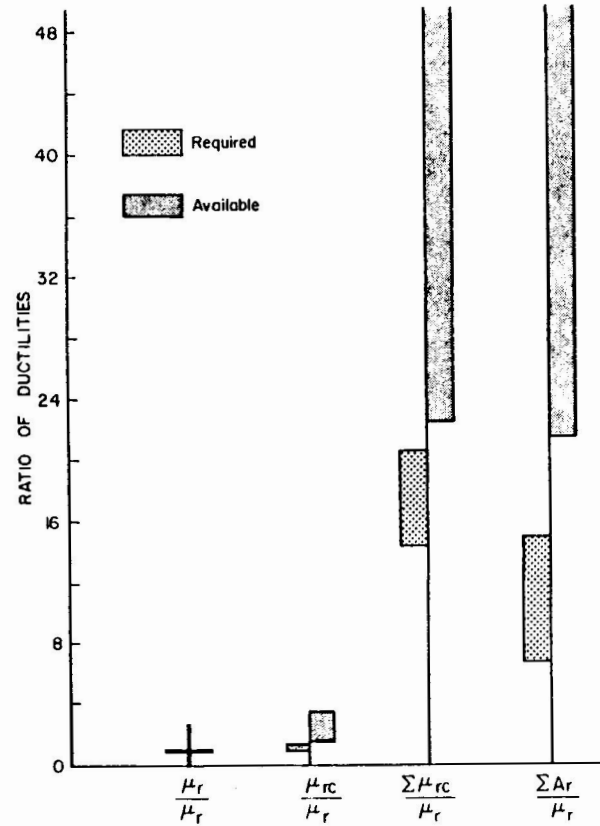
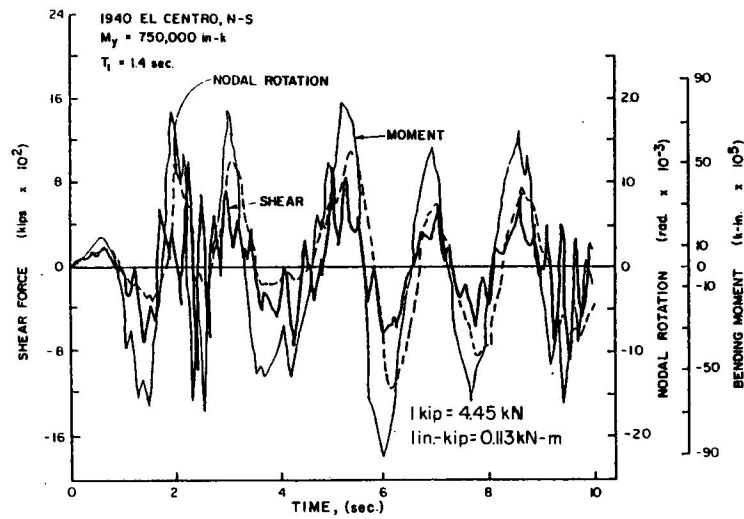
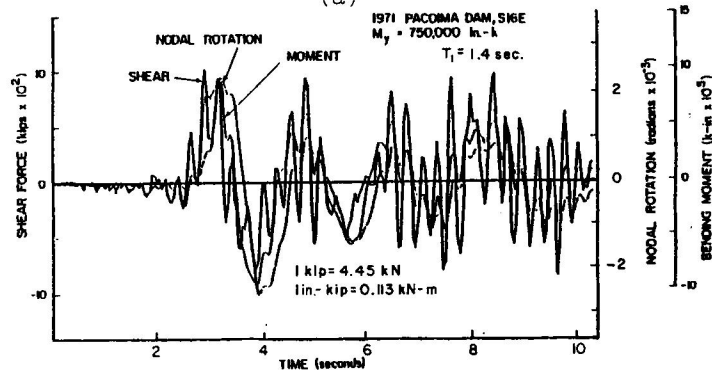


Fig. 33 Comparison of Ratios of Maximum Ductility Required with Corresponding Ratios of Available Ductilities - Using Rotational Ductility,  $\mu_r$ , as the Reference Measure



(a)



(b)

Fig. 34 Relative Variation with Time of Shear Moment and Rotation in Hinging Region - 20-Story Isolated Wall